EFFECT OF DIFFERENT OPERATING CONDITIONS ON THE SENSITIVITY OF NONINVASIVE METHODS TO DETECT CRYSTALLIZATION FOULING IN LIQUID-TO-AIR MEMBRANE ENERGY EXCHANGERS

B. Xing[1], A. O. Olufade[2] and C. J. Simonson[1]

[1] Department of Mechanical Engineering, University of Saskatchewan, 57 Campus Dr., Saskatoon, SK S7N 5A9, CANADA, bix547@ usask.ca

[2] ACCURASEE INSTRUMENTS, 229 – 116 Research Dr., Saskatoon, SK S7N3R3, CANADA

ABSTRACT

Liquid-to-air membrane energy exchangers (LAMEEs) can use membranes to transfer both heat and moisture in heating, ventilating and air-conditioning (HVAC) systems to provide air at a comfortable temperature and humidity to buildings. However, research has shown that crystallization fouling significantly degrades the performance of LAMEEs. The ability to early detect the onset of fouling is, therefore, desirable as remedial measures can be taken to prevent the accumulation of deposits in operating LAMEEs.

The primary objective of this paper is to assess the effect of two operating conditions on the sensitivity of two noninvasive methods to detect the onset of crystallization fouling in a LAMEE. The methods are based on the analysis of uncertainty and rate of change of overall moisture transfer resistance of the LAMEE. To increase the sensitivity of the methods, the membrane surface area is doubled (to increase the rate of moisture transfer through the membrane) and/or the mass flow rate of air flowing into the LAMEE is halved.

The main finding from the paper is that increasing the membrane area and/or decreasing the mass flow rate of air can improve the sensitivity of the methods to detect the onset of fouling in the LAMEE.

INTRODUCTION

HVAC (heating, ventilating, and air conditioning) systems are important in modern buildings since they provide thermal comfort for occupants. In addition, HVAC systems account for approximately one-fifth of global energy consumption [1].

Liquid-to-air membrane energy exchangers (LAMEEs), which use membranes to simultaneously transfer heat and moisture between liquid and air in order to condition air, have primarily been developed to reduce energy consumption in HVAC systems [2]. LAMEEs can also reduce the operating costs of HVAC systems and minimize CO_2 emissions [3-5]. However, since LAMEEs make use of salt solutions, crystallization fouling may occur on the membrane and reduce the effectiveness of the LAMEE.

The methods that are used to detect the onset of fouling can be classified as either invasive or noninvasive [6]. Invasive methods require equipment to be disassembled for fouling to be physically examined or observed. On the other hand, non-invasive methods do not disrupt equipment operation [6].

There are a few studies on crystallization fouling in LAMEEs for HVAC applications in the literature. Charles and Johnson [7] studied crystallization in hollow-fiber membranes with different media, such as $CaCO_3$(aq), $CaSO_4$(aq) and tap H_2O(aq), using a fouling factor. Crawford and Silva [8] assessed the impact of crystallization fouling on a membrane-based cooling system by monitoring the rate of moisture transfer through the membrane. Although, the two studies [7, 8] reported the effect of fouling on the performance of the exchangers tested, neither of them determined the onset of fouling in the experiments reported.

Olufade and Simonson [9-11] applied invasive and noninvasive methods to detect the onset of crystallization fouling in a LAMEE that was fouled using $MgCl_2$(aq). They found that both invasive (membrane autopsy) and noninvasive (direct observation of membranes using a microscope) methods that are based on direct measurements are more sensitive to detect the onset of fouling than noninvasive methods that are based on indirect measurements (e.g., moisture transfer resistance). They also reported that both the bulk supersaturation of a solution and the relative humidity of air combine to influence the onset and severity of crystallization fouling in the LAMEE.

In this paper, the work performed by Olufade and Simonson [9] is further explored by evaluating the effect of two operating conditions on the sensitivity of two noninvasive methods to detect the onset of crystallization fouling in a LAMEE.

ISBN: 978-0-9984188-1-0; Published online www.heatexchanger-fouling.com

EXPERIMENTS

Test facility

The test facility that was developed by Olufade [6] to study fouling in LAMEEs is used for the experiments performed and reported in this paper. A modified schematic of the test facility is shown in Fig. 1.

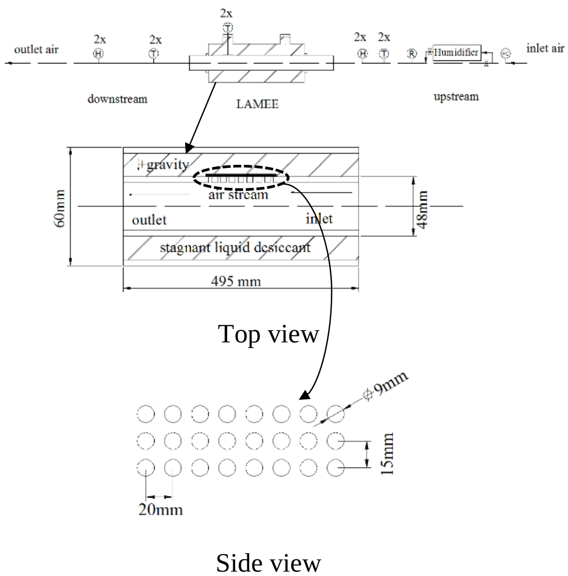

Fig. 1. Schematic of the test facility (adapted from Ref. [6]).

Fig. 1 shows that air is conditioned and delivered to the test section (LAMEE) at a controlled relative humidity and mass flow rate. The properties of the bulk air stream at the inlet and outlet of the LAMEE are measured to calculate the moisture transfer resistance across the LAMEE. The changes in resistance serve a possible indicator of crystallization fouling in the membrane.

The LAMEE is a shell-and-tube exchanger with an impermeable tube that is perforated with 24 holes (i.e., an additional 12 holes compared to the tube used in a previous test facility [6] to double the exposed membrane area). A semi-permeable membrane is attached to the outside of the impermeable tube to prevent the salt solution on the shell side from entering the tube while allowing moisture transfer between the air and salt solution via holes that are drilled through the tube. The salt solution on the shell side of the LAMEE is stagnant.

The membrane used in this paper is of the same material as the one used in Olufade and Simonson [9] (i.e., expanded polytetrafluoroethylene laminates as reported in Ref. [12]). The membrane area in this study is 1.53×10^{-3} m^2, which is twice the membrane area used in Olufade and Simonson [9]. The uncertainty in the membrane area is assumed to be ±1% whereas the uncertainty was assumed to be ±5% in Olufade and Simonson [9].

Operating conditions

The tests reported in this study are conducted at room temperature (20 – 24ºC). It should be noted that large temperature discrepancy is avoided between different tests since temperature can affect moisture transfer capability of the LAMEE. A supersaturated $MgCl_2$ desiccant solution with C* = 1.03 is used in the LAMEE (C* is the normalized solution concentration relative to the saturation concentration at the same temperature). The tests are conducted using two mass flow rates of air, i.e. 0.7×10^{-5} kg/s and 1.4×10^{-5} kg/s.

METHODOLOGY

Characterization of fouling

Since moisture transfer is the main driving force in the LAMEE, fouling is characterized by moisture transfer resistance (R). The resistance is calculated using:

$$R = \frac{\Delta W_{lm}}{\dot{m}''_v} \qquad (1),$$

where the log-mean humidity ratio difference, ΔW_{lm}, is given by:

$$\Delta W_{lm} = \frac{W_{air,out} - W_{air,in}}{\ln\left(\frac{W_{sol} - W_{air,in}}{W_{sol} - W_{air,out}}\right)} \qquad (2),$$

where $W_{air,in}$, $W_{air,out}$ and W_{sol} are the humidity ratio of inlet air, outlet air and air in equilibrium with the solution at the membrane interface, respectively.

The moisture flux through the membrane ($\dot{m}''_v$) is given by:

$$\dot{m}''_v = \frac{\dot{m}_{air}\left(W_{air,out} - W_{air,in}\right)}{A_{mem}} \qquad (3),$$

where $\dot{m}_{air}$ is the mass flow rate of air and A_{mem} is the surface area of the membrane.

If the LAMEE is operated at non-fouling conditions, e.g. using distilled $H_2O(aq)$, its moisture transfer resistance will be constant during a test except for fluctuations due to random error (see Fig. 2). Fouling may, therefore, be concluded if there is an increase in the moisture transfer resistance of the LAMEE during a test. An increase in the resistance of the LAMEE can be explained to arise from the blocking of the membrane pores which limits the moisture transfer rate.

Transient period

As shown in Fig. 2, the resistance decreases during the first few minutes of a test. This period can be defined as a transient period where the boundary conditions of the LAMEE are changing. A test is therefore considered to be at steady state (with respect to the boundary conditions and **not** fouling) when the boundary conditions stabilize.

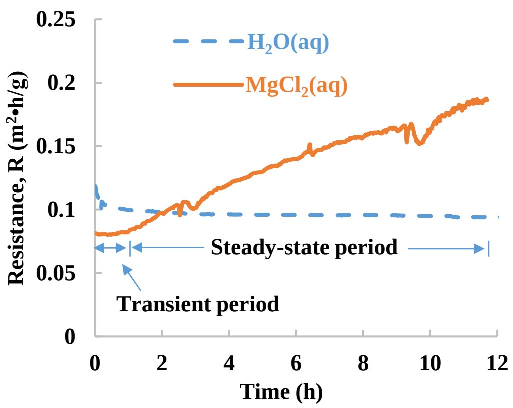

Fig. 2. Moisture transfer resistance across the LAMEE for tests performed using distilled H_2O(aq) and $MgCl_2$.

In Fig. 2, the resistance of the LAMEE is compared for tests performed using distilled H_2O(aq) versus $MgCl_2$(aq). The transition from transient to steady state is identified for both tests as the point where the slope of the resistance reaches zero. It should be pointed out that the initial discrepancy between the two resistance graphs is due to the difference in solution-side boundary conditions. It can be seen that the resistance doubles during the test with $MgCl_2$(aq) as compared to the negligible change that is observed in the test with distilled H_2O(aq).

Detection of fouling

As previously mentioned, two noninvasive methods (i.e., uncertainty and slope) are applied to detect the onset of fouling in the LAMEE. In both methods, the resistance across the LAMEE is analyzed using a moving window that starts from a fixed point at the start of the steady-state period and extends to an end point that incrementally moves towards the end of the test at 12 h.

Uncertainty method

According to the uncertainty method, the onset of fouling is confirmed [6] when an increase in resistance is greater than the uncertainty at a 95% confidence interval, as shown in:

$$f_u = \left| \frac{R_i - R_o}{U_{R_i - R_o}} \right| > 1 \qquad (4).$$

The uncertainty of resistance (U_R) depends on membrane area (A_{mem}), mass flow rate of air ($\dot{m}_{air}$), humidity difference between inlet and outlet air streams (ΔW), and log-mean humidity difference (ΔW_{lm}) as given by:

$$\frac{U_R}{R} = \sqrt{\left(\frac{U_{A_{mem}}}{A_{mem}}\right)^2 + \left(\frac{U_{\dot{m}_a}}{\dot{m}_a}\right)^2 + \left(\frac{U_{\Delta W}}{\Delta W}\right)^2 + \left(\frac{U_{\Delta W_{lm}}}{\Delta W_{lm}}\right)^2} \qquad (5).$$

Theoretically, increasing the membrane surface area (A_{mem}) can reduce the uncertainty to detect fouling in the LAMEE. This is because the moisture transfer rate through the membrane can be increased by increasing the membrane area. The increase in moisture transfer rate is expected to increase the difference in humidity ratio between the inlet and outlet air streams (ΔW) and reduce the overall uncertainty in resistance (R).

Slope method

For the slope method, the onset of fouling is the point where the slope of resistance from the start of steady state to a moving point exceeds its random uncertainty at a 95% confidence interval [6]:

$$f_{sl} = \left| \frac{Slope_{R_o \to R_i}}{P_{Slope_{R_o \to R_i}}} \right| > 1 \qquad (6).$$

The random uncertainty in the slope is a product of the Student t-value and the standard error of the slope:

$$P_{Slope_{R_o \to R_i}} = t \times SEE \qquad (7).$$

The slope and standard error of resistance (SEE) are estimated using the “LINEST” function in Microsoft Excel [13].

RESULTS AND DISCUSSION

The rate of change of resistance during a test is shown in Fig. 3 for moving windows of 10, 20, 30 and 40 data points. As the size of the moving window

ISBN: 978-0-9984188-1-0; Published online www.heatexchanger-fouling.com

increases, the plots of the slope of resistance smoothen out. Initially (before 40 min), the slope of resistance is negative but transitions to a value of 0 at 42 min which is the start of the steady-state period (i.e., the end of the transient period).

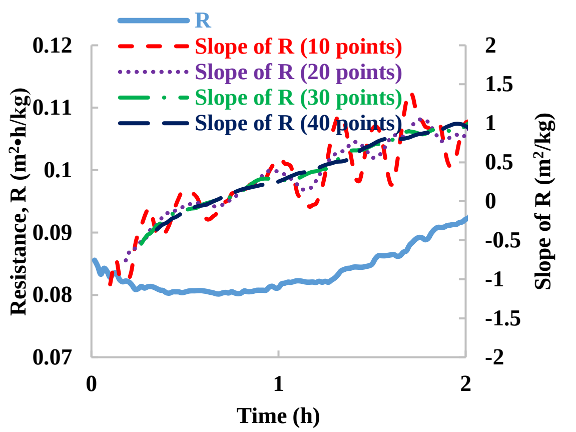

Fig. 3. Resistance of the LAMEE and the slope of resistance as a function of time for a test using $MgCl_2$ at C* = 1.03, RH = 10%, and air flow rate of 1.4×10^{-5} kg/s.

It is observed from Fig. 4 that the uncertainty in resistance increases with time because of crystallization fouling in the membrane. The uncertainty method is unable to detect fouling in the test since the increased resistance does not exceed the uncertainty (i.e., $f_u < 1$), which agrees with the results of Olufade and Simonson [9] for the same test conditions and membrane but with 50% of the membrane surface area. The slope method, on the other hand, detects fouling right after the end of the transient period in both studies (i.e., $f_{sl} > 1$). It should be noted that the presence of crystallization fouling has been verified at this test condition using scanning electron microscopy and digital microscopy [11].

The relative uncertainty in the resistance of the LAMEE at the start of steady state is 38% which is the essentially the same as 40% for Olufade and Simonson [9]. The uncertainty in resistance is not reduced in the current test (Fig. 4) because the increase in resistance ($0.11 m^2 \bullet kg/h$) during the test is not sufficient to exceed its corresponding uncertainty. Therefore, fouling is not detected using the uncertainty method despite a doubling of the membrane surface area.

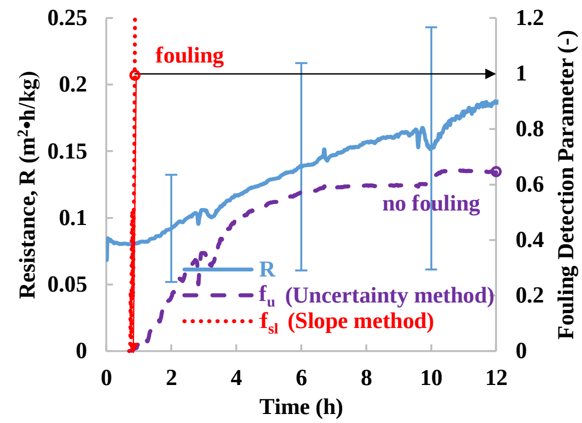

Fig. 4. Resistance of the LAMEE and fouling detection parameters (i.e., f_u and f_{sl}) for a test using $MgCl_2$ at C* = 1.03, RH = 10%, and air flow rate of 1.4×10^{-5} kg/s.

Figs. 5 and 6 present the results of a test at the same condition as the test in Figs. 3 and 4 but with a 50% lower mass flow rate of air.

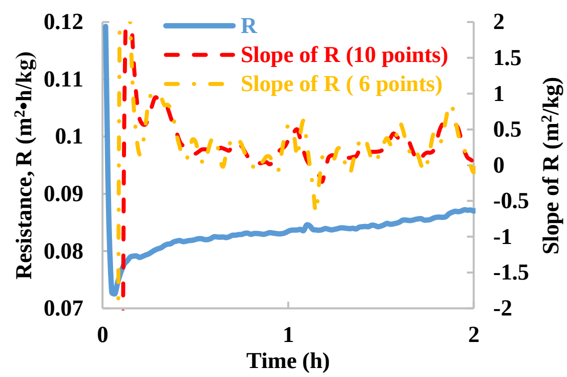

Fig. 5. Resistance of the LAMEE and the slope of resistance as a function of time for a test using $MgCl_2$ at C* = 1.03, RH = 10%, and air flow rate of 0.7×10^{-5} kg/s.

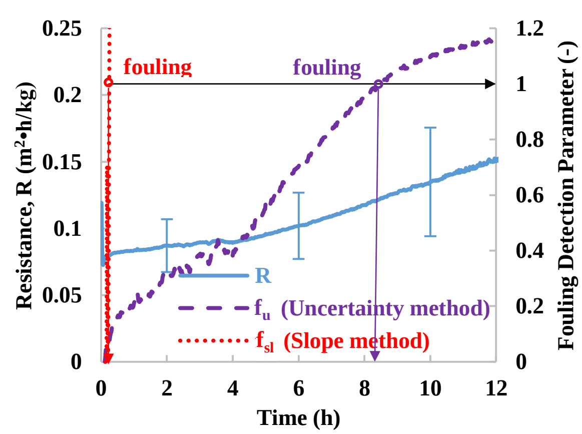

Fig. 6. Resistance of the LAMEE and fouling detection parameters (i.e., f_u and f_{sl}) for a test using

ISBN: 978-0-9984188-1-0; Published online www.heatexchanger-fouling.com

$MgCl_2$ at C* = 1.03, RH = 10%, and air flow rate of 0.7×10^{-5} kg/s.

Fig. 5 shows that the start of steady state begins much earlier (8 min in Fig. 5 compared to 42 min in Fig. 3). It should be noted that increasing the size of the moving window in Fig. 5 also smoothens the plot of resistance as was seen in Fig. 3. Fig. 6 indicates that the uncertainty method detects the onset of fouling at 8.5 h whereas the slope method detects fouling at 9 min. The increased resistance exceeds corresponding uncertainty in this test, regardless the fact that less fouling forms (resistance increases by 0.07 m^2•kg/h in this test, whereas resistance increases by 0.11m^2•kg/h in the test with doubled flow rate).

A comparison of the results obtained in this paper and that of Olufade and Simonson [9] is presented in Table 1.

Table 1. Comparison of results between this paper and Olufade and Simonson [9].

Parameter	This paper		Olufade and Simonson, [9]
$\dot{m}_{air} \times 10^{-5}$ (kg/s)	0.7	1.4	1.4
$A_{mem} \times 10^3$ (m^2)	1.53		0.76
W_{in} ($g_v/kg_{dry\ air}$)	1.9	1.8	1.8
W_{out} ($g_v/kg_{dry\ air}$) [supersaturated $MgCl_2$ test]	3.8	2.8	2.4
W_{out} ($g_v/kg_{dry,\ air}$) [$H_2O(aq)$ test]	8.2	5.1	4.3
U_R at the start of steady state (%)	24	38	40
Fouling detection time for the uncertainty method (h)	8.5	–	–
Fouling detection time for the slope method (h)	0.15	0.72	2.5
Increased R over experimental period (m^2•h/kg)	0.07	0.11	0.11

Table 1 shows that doubling the membrane surface area alone neither significantly reduces the uncertainty in resistance nor the time to detect fouling for the uncertainty method. However, the time to detect fouling is reduced for the slope method (e.g., 0.7 h in this paper as compared to 2.5 h in Ref. [9]). On the other hand, doubling the membrane area and halving the air mass flow rate noticeably decreases both the uncertainty in resistance and fouling detection time for both methods.

CONCLUSION

The main aim of this paper is to assess the effect of two operating conditions on the sensitivity of two noninvasive methods (i.e., uncertainty and slope) to detect the onset of crystallization fouling in a liquid-to-air membrane energy exchanger (LAMEE). To achieve this objective, the surface area of the membrane used in a previously tested LAMEE was doubled and the mass flow rate of air was halved.

The major conclusion in this study is that reducing the uncertainty in the measured resistance of the membrane (by increasing membrane area and/or decreasing the air flow rate) can increase the sensitivity to detect the onset of fouling in the LAMEE.

NOMENCLATURE

Roman

A_{mem}	Membrane area, m^2
C*	Normalized solution concentration, –
f_u	Criterion for fouling detection for the uncertainty method, –
f_{sl}	Criterion for fouling detection for the slope method, –
$\dot{m}''_v$	Moisture flux through the membrane, g·m^2/h
$\dot{m}_{air}$	Mass flow rate of air, kg/s
P	Random uncertainty, –
R	Moisture transfer resistance, m^2·h/kg
R_i	Moisture transfer resistance of a moving point, m^2·h/kg
R_o	Moisture transfer resistance at the start of the steady-state period, m^2·h/kg
RH	Relative humidity of air, %
Slope of R	Slope of resistance, m^2/kg
$Slope_{R_o \to R_i}$	Slope of the difference between the moisture transfer resistance at the start of the steady-state period and a moving point , m^2/kg
t	t-Student statistic, –
$W_{air,in}$	Inlet air humidity ratio, $g_v/kg_{dry\ air}$
$W_{air,out}$	Outlet air humidity ratio, $g_v/kg_{dry\ air}$
W_{sol}	Humidity ratio of air in equilibrium with the solution at the membrane interface, $g_v/kg_{dry\ air}$
ΔW	Difference in humidity ratio between the inlet and outlet air streams, $g_v/kg_{dry\ air}$
ΔW_{lm}	Log-mean humidity ratio, $g_v/kg_{dry\ air}$

Subscript/Superscript

ISBN: 978-0-9984188-1-0; Published online www.heatexchanger-fouling.com

air Air
in Inlet of the LAMEE
out Outlet of the LAMEE
sol Desiccant solution
v Water vapor

REFERENCES

[1] Perez-Lombard L., Ortiz J., Pout C., A review of buildings energy consumption information, *Energy and Buildings*, vol. 40, pp. 394-398, 2008.

[2] Ge G., Abdel-Salam M. R. H., Besant R. W., Simonson C. J., Research and applications of liquid-to-air membrane energy exchangers in building HVAC systems at University of Saskatchewan: A review, *Renewable and Sustainable Energy Reviews*, vol. 26, pp. 464-479, 2013.

[3] Abdel-Salam A. H., Ge G., Simonson C. J., Performance analysis of a membrane liquid desiccant air-conditioning system, *Energy and Buildings*, vol. 62, pp. 559-569, 2013.

[4] Abdel-Salam A. H., Simonson C. J., Annual evaluation of energy, environmental and economic performances of a membrane liquid desiccant air conditioning system with/without ERV, *Applied Energy*, vol. 116, pp. 134-148, 2014.

[5] Abdel-Salam A. H., Ge G., Simonson C. J., Thermo-economic performance of a solar membrane liquid desiccant air conditioning system, *Solar Energy*, vol. 102, pp. 56-73, 2014.

[6] Olufade, A.O., Experimental characterization of crystallization fouling in liquid-to-air membrane energy exchangers, Ph.D. Thesis, Department of Mechanical Engineering, University of Saskatchewan, 2018.

[7] Charles N. T., Johnson D. W., The occurrence and characterization of fouling during membrane evaporative cooling, *Journal of Membrane Science*, vol. 319, pp. 44‑53, 2008.

[8] Crawford R., da Silva A. K., Experimental testing of a passive, evaporation-based roof cooling system, *Energy Buildings*, vol. 71, pp. 12‑19, 2014.

[9] Olufade A.O., Simonson C.J., Application of indirect non-invasive methods to detect the onset of crystallization fouling in a liquid-to-air membrane energy exchanger, *International Journal of Heat and Mass Transfer*, vol. 92, pp. 33-45, 2018.

[10] Olufade A.O., Simonson C.J., Detection of crystallization fouling in a liquid-to-air membrane energy exchanger, *Experimental Thermal and Fluid Science*, vol. 127, pp. 663-673, 2018.

[11] Olufade A.O., Simonson C.J., Characterization of the evolution of crystallization fouling in membranes, *ACS Omega*, vol. 3, no. 12, pp. 17188-17198, 2018.

[12] Beriault D. E., Run-around membrane energy exchanger prototype 4 design and laboratory testing, M.Sc. Thesis, Department of Mechanical Engineering, University of Saskatchewan, 2011.

[13] Microsoft, LINEST function, https://support.office.com/en-us/article/linest-function-84d7d0d9-6e50-4101-977a-fa7abf772b6d, 2019 (last accessed February 18, 2019).